Optimal Routing and Ecological Driving Systems for EVs/HEVs

by

Bowen Zhang

A thesis submitted in partial fulfillment
of the requirements for the degree of
Master of Science in Engineering
(Electrical Engineering)
in the University of Michigan-Dearborn
2017

Master's Thesis Committee:

Assistant Professor Wencong Su, Chair
Associate Professor Hua Bai
Assistant Professor Mengqi Wang

DEDICATION

This edition of the Master's Thesis by Bowen Zhang, "ROUTING AND ECOLOGICAL DRIVING OPTIMIZATION OF ELECTRIC VEHICLES AND HYBRID ELECTRIC VEHICLES", is dedicated to all the professionals, students and people who are working on or interested in renewable energy, electric vehicle routing and charging, vehicle economic operation and power management.

ACKNOWLEDGEMENTS

Foremost, I would like to express my deepest gratitude to my parents, Liwu Zhang and Yili Huang. Their love and support mean a lot to me.

My significant gratitude goes to my thesis advisor, Dr. Wencong Su, who has provided me guidance and encouragement since I started my master degree studies. I greatly appreciated our discussion of my master thesis and other research topics. It was a great pleasure having the opportunity to work with him.

My sincere thanks also go to my lab mates and other friends, who help and support me all the time. You provided me many great ideas and suggestions. We not only worked together but shared life with each other.

Last but not least, I would like to thank my thesis committee members: Professor Kevin (Hua) Bai, and Professor Mengqi (Maggie) Wang, for their attendance for my thesis defense and insightful advice.

TABLE OF CONTENTS

LIST OF FIGURES

LIST OF TABLES

LIST OF ABBREVIATIONS

EV	Electric Vehicle
SOC	State of Charge
PDP	Pick-up and Delivery Problem
HEV	Hybrid Electric Vehicle
EDA	Estimation of Distribution Algorithm
GA	Genetic Algorithm

ABSTRACT

Nowadays, there has been an unprecedented growth of energy demand and environmental concerns, in terms of the vehicle emissions and fuel efficiency. Transportation electrification is seen as an effective way to substantially satisfy both requirements. By applying the secondary electric power source, Electric Vehicles (EVs) and Hybrid Electric Vehicles (HEVs) become the promising solutions, and have potential to revolutionize urban transportation systems. Therefore, the pre-trip planning and power management problems regarding EVs and HEVs have attracted many researchers' attention. However, there is little work addressing the EV/HEV fuel economy with the consideration of detailed vehicle powertrain model and meet the constraints from various perspectives. To address these challenges, on one hand, we propose a simulation framework for the economic operation of pure EV considering dynamic electricity price. We address optimal routing and charging problems of Uber-like EV considering dynamic electricity price and passenger satisfaction. It aims not only at finding the best route over a finite driving cycle, but also optimizing the EV charging behavior, in order to achieve optimal fuel efficiency and reduce cost. On the other hand, the detailed powertrain model for the individual power-split HEV is proposed. Constraints from vehicle power flows, road conditions, and speed limits are included. Two stochastic methods, the generic algorithm (GA) and the estimation of distribution algorithm (EDA) are implemented to verify the feasibility, accuracy, robustness, and effectiveness of the proposed methods. Moreover, the proposed models for individual EV/HEV can be further tailored and extended to multiple considering other emerging technologies (e.g., connected and automated vehicles) in the near future.

Chapter 1
Introduction

1.1. Background

In the last few decades, an emphasis on green technology is greatly demanded by modern cities. Today, 54% of the world's population lives in urban areas, a proportion that is expected to 66% by 2050 [1]. Besides, the significant growth of city infrastructures has led to an ever-increasing usage of transportation, resulting in severe pollution and other environmental issues [2]. The U.S. government has made huge efforts to develop the transportation electrification technologies, and advances in intelligent transportation systems and smart grid technologies offer great promise to widely popularize electric vehicles (EVs) and hybrid electric vehicles (HEVs) because of their low emissions, alternative energy source, and high fuel economy.

With the emerging transportation network services, such as Uber, Lyft, and Curb, EVs and HEVs can act as innovative transportation tools. This brings both potential benefits and challenges. Beside the driving route optimization, the vehicle charging plan should also be considered when EVs and HEVs are utilized as carriers. In terms of their fuel consumption, it depends on various factors, such as the characteristics of the drivetrain, operation conditions according to road and traffic conditions, and driving patterns. Therefore, EV and HEV drivers need to be assisted technologically in operating the vehicle under the fuel efficient conditions [3]. This is called the ecological driving, and many studies have been conducted on this topic.

1.2. Objective of Thesis

The objective of this research is to propose a detailed mathematical model for optimal routing and charging of an individual Uber-like EV, and a powertrain model of individual power-split HEV, and explore their optimal driving and charging information.

For the Uber-like EV, dynamic electricity price and passenger satisfaction are taken into consideration. The driver will make different route decisions considering the electricity prices at every charging station and passengers' preferences, such as less travel time, or less travel distance.

For the power-split HEV, the purpose is to achieve a better vehicle fuel efficiency and optimize the HEV speed profile over a finite driving cycle under the distance domain. The battery state-of-charge (SOC) information is also generated. To demonstrate the feasibility, accuracy, robustness and effectiveness of the proposed HEV model, a stochastic method called estimation of distribution algorithm (EDA) is utilized for solving the nonlinear and constrained objective function.

1.3. Organization

The Introduction about the whole master thesis was presented in chapter 1. Chapter 2 was based on the publication [4], and it presented a detailed mathematical model of an Uber-like EV, together with several case studies under different circumstances. Chapter 3 proposed a distance-based long term optimization of a power-split HEV was proposed to optimize the vehicle speed and SOC profiles over the entire driving cycle, by utilizing the EDA method. The section 4 concluded the whole contributions of the entire research work.

1.4. References

[1] Dep. Economic and Social Affairs, "World Urbanization Prospects, The 2014 Revision Highlights", United Nations, New York, 2014

[2] M. A. Hannan, F. A. Azidin, & A. Mohamed (2014). Hybrid electric vehicles and their challenges: A review. *Renewable and Sustainable Energy Reviews*, *29*, 135-150

[3] D. L. Greene, H. H. Baker, Jr., and S. E. Plotkin, "Reducing greenhouse gas emissions from U.S. Transportation," Center for Climate and Energy Solutions, 2011

[4] B. Zhang, T. Chen, and W. Su, "Optimal Routing and Charging of Uber-like Electric Vehicle Considering Dynamic Electricity Price and Passenger Satisfaction", *2016 IEEE Transportation Electrification Conference and Expo Asia-Pacific*, Busan, Korea, June 1-4, 2016

Chapter 2

Optimal Routing and Charging of an Uber-like Electric Vehicle Considering Dynamic Electricity Price and Passenger Satisfaction

This chapter explores and presents a detailed mathematical model for optimal routing and charging of an Uber-like electric vehicle (EV) taking into account dynamic electricity price and passenger satisfaction. Based on an extended Pickup and Delivery Problem (PDP), the proposed optimization problem aims at the determination of the best route from the start node (origin) to the end node (final destination) while satisfying the requirements of all passengers (e.g., travel time and travel distance), together with reducing the driver's operation cost (e.g., electricity charging cost). The proposed model can be extended and developed into multi-vehicle optimal routing and charging problems.

2.1. Introduction

The pick-up and delivery problem (PDP) has been one of the most studied network logistic problems in the last decade. It can be depicted as searching the optimal route under several transportation requests to a fleet of vehicles, by minimizing a specific objective function which is subject to a variety of constraints [1]. A transportation request consists of picking up a certain number of passengers from predetermined pick-up locations and dropping them off at predetermined delivery locations respectively [2].

Meanwhile, the electric vehicles (EVs) are increasingly connected to electric utilities over the next few decades. Advances in intelligent transportation systems and smart grid technologies offer great promise to widely popularized EVs and have potential to revolutionize urban transportation systems [3]. The EV is not only a transportation tool but also an electrify carrier. It can achieve high energy efficiency, reduce carbon emissions, spur high-technology innovation, and ensure a reliable energy supply [4]. The U.S. administration intends again to reform the transportation service, aiming at reducing emissions and decreasing dependence on fossil oil, setting a target that 50% of new car sales will be EVs by the year of 2050 [5]. The California Air resources Board, the states of Massachusetts and New York, are requiring ‘zero emission vehicles (ZEVs) as a pollution prevention strategy [6]. The electrification of transportation brings both opportunities and challenges to existing infrastructures.

Also, the emerging transportation network services, such as Uber, Lyft, and Curb, have resulted in operational disruptions and innovations in the United States, ultimately increasing occupancy and reducing traffic congestion [7]. These innovations enable the sharing of vehicular resources via a variety of mobile apps, ultimately shifting the urban mobility modes from private vehicles to the dynamic transportation services.

However, there is very little work on addressing the coupled challenges of EV charging and Uber-like vehicle routing problems. If successfully implemented together, an ever-increasing number of Uber-like electric vehicle services will radically change the traditional views of the power and transportation industries, the social environment and the business world [8].

Most current researches focus on EV charging control and assume the EV parking time is much longer than its charging time [9]. However, in our scenarioes, the EV should charge immediately after arriving at any charging station if it is assigned to charge at the particular charging station. Because the selected EV model in our proposed service framework just has a very small battery capacity and cannot wait for a long time in the middle of the trip before finishing the customer service.

It is also noteworthy that the PDP with considering EV participation is not a pure routing problem or constrained shortest path problem [10], [11] , since our aims are not only finding the best route, but also implementing the optimization of the EV charging behavior.

Therefore, the objective of this chapter is to explore and propose a detailed mathematical model for optimal routing and charging of an Uber-like EV, taking into account dynamic electricity price and passenger satisfaction. The contributions of this chapter are summarized as follows:

(1) Propose a detailed mathematical model of one single frequently charged EV;

(2) Investigate the impact of electricity prices at different charging stations on the optimal route decision made by the EV driver;

(3) Discuss the different route selections when passengers' preferences and requirements vary under certain circumstances;

(4) Discuss the future research trends and the potential equilibrium between the transportation network distribution and city power system.

The remainder of this chapter is organized as follows: Section II presents the problem formulation that is built upon the extended PDP problem. Section III introduces the case studies, including three different scenarios. Section IV presents the conclusions and future works.

2.2. System Formulation

In this section, we mainly concentrate on formulating the framework of the extended PDP. From an EV driver's perspective, the passengers submit their request (i.e., pick-up and delivery locations) which are transferred to the driver via mobile app such as Uber. Our proposed optimization problem will be solved and determine the best route for the driver, from the start node (origin) to the end node (final destination) to satisfy the requirements of all passengers (e.g., total travel time and total travel distance), while reducing the driver's operation cost (e.g., electricity charging cost).

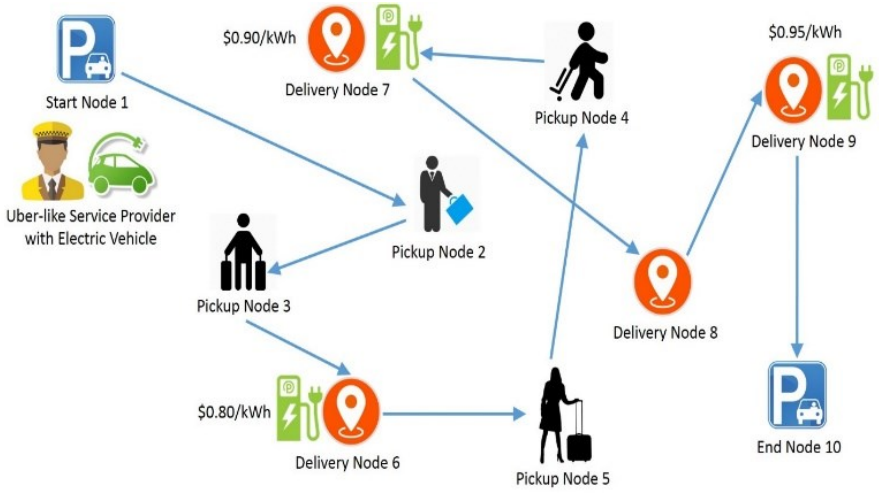

Figure 1. An illustrated 10-node example

Figure 1 illustrates a simple 10-node example with 1 start node, 4 pick-up nodes, 4 delivery nodes and 1 end node. The blue arrows illustrate one feasible solution to carrying 4 passengers from their desired locations to respective destinations. The EV charging stations are available at a certain locations with dynamic prices.

It is important to note that there are no direct relations among charging nodes, pick-up nodes and delivery nodes. Charging stations are pre-defined at certain locations according to

the real city transportation network.

Also, the proposed optimization problem is different from the traditional pick-up and delivery problem. Because an EV may need to be recharged before arriving at pick-up and delivery nodes. The dynamic charging price will affect the driver's decisions on either the optimal route choice or the time and method to recharge vehicle batteries. On the other hand, these decisions will affect the level of passenger satisfaction (e.g., travel distance and time), and ultimately change the driver's benefits (e.g., income and reputation) [12].

The mathematical model mainly concentrates on minimizing passengers' total travel distance, total travel time and electricity charging cost, subject to local and global constraints. Therefore, there are three parts included in the final objective function as expressed in Equation (1). The weighing terms can be adjusted based on the passenger preferences and dynamic changes of electricity prices at different charging stations.

$$\min M = \omega_1 \left[\sum_{i,j \in N} d_{ij} x_{ij} \right] + \omega_2 \left[\sum_{\substack{d \in D \\ p \in P \\ i \in U}} q_i \left(t_d - t_p \right) \right] + \omega_3 \left[\sum_{\substack{i \in N \\ j \in C}} x_{ij} \lambda_i Q_i t_{C,i} \right] \tag{1}$$

Subject to

$$\sum_{j \in P \cup D \oplus \{e\}} x_{ij} = 1, \forall i \in \{s\} \tag{2}$$

$$\sum_{i \in P \cup D \oplus \{s\}} x_{ij} = 1, \forall j \in \{e\} \tag{3}$$

$$t_1 = 0 \tag{4}$$

$$\sum\nolimits_{j \in P \cup D \oplus \{e\}} x_{ij} \leq 1, \forall i \ \in N \backslash (\{s\} \oplus \{e\}) \tag{5}$$

$$\sum\nolimits_{i \in P \cup D \oplus \{s\}} x_{ij} \leq 1, \forall j \ \in N \backslash (\{s\} \oplus \{e\}) \tag{6}$$

$$-\mathrm{M}(1 - x_{ri}) \leq \sum_{j \in N} \left(x_{ij} - x_{ri} \right) \leq M(1 - x_{ri}), \tag{7}$$

$$\forall r \in \backslash\{e\}, \forall i \in N \backslash (\{s\} \oplus \{e\})$$

$$-M(1 - x_{rj}) \leq \sum_{i \in N} (x_{ij} - x_{rj}) \leq M(1 - x_{rj}), \tag{8}$$

$$\forall r \in N \backslash \{s\}, \forall j \in N \backslash (\{s\} \oplus \{e\})$$

$$t_p - t_d < M(1 - q_i), \forall p \in P, \forall d \in D \tag{9}$$

$$-M \sum_{i \in N} x_{ij} \leq t_{C,j} \leq M \sum_{i \in N} x_{ij}, \forall j \in C \tag{10}$$

$$-M(1 - x_{ij}) \leq z_i - z_j - \frac{E_{ij}}{E_{max}} + \frac{Q_i t_{C,i}}{E_{max}} \leq M(1 - x_{ij}), \tag{11}$$

$$\forall i, j \in N$$

$$Z_{min} \leq z_i \leq Z_{max}, \forall i \in N \tag{12}$$

$$x_{ij} \in \{0,1\}, t_i \geq 0, t_{C,i} \geq 0, \forall i, j \in N \tag{13}$$

$$t_{ij} = t_{ij}^{Free} \left(1 + \alpha \left(\frac{V}{C}\right)^{\beta}\right), \forall i, j \in N \tag{14}$$

According to some basic transportation requirements for a traffic route, Equation (2) indicates each node must have only one path leading away from it while Equation (3) implies each node must have only one way leading to it. Equation (4) sets the reference time for the start node to be zero.

If the left hard sides of Equation (5) and (6) are equal to one, it means the EV passes through that node during the trip. We use the big *M* method to describe some constraints, as from Equations (7)-(11). The EV charger is only available at a certain locations. The value of q depends on the charging methods (e.g., uncontrolled, wireless, or smart charging). Here, for the sake of simplicity, q can be assumed to be a constant across all types of node, as stated in the objective function.

Equations (7) and (8) indicate if the EV enter or leave a node that is neither the start node nor the end node, then it must lead away from (to) this node afterward (beforehand). The pick-

up time should always be prior to the delivery time, as stated in Equation (9). In Equation (10), the EV charging time is set to be zero if it does not stop by a charging station. The SOC requirement is stated in Equation (12). For example, the SOC should be within a specific range at any node. We set $Z_{min} = 0.1$ as the lower limit and $Z_{max} = 0.9$ as the upper limit. The travel time between nodes i and j should be determined by a function of distance and other factors, such as the driving speed, road conditions and weather. Equation (14) shows the revised function with other considerations, including the density of intersections and the traffic flow in a given metropolis [13]. The parameter t_{ij}^{Free} stands for the free flow time from the node i to the node j, V for traffic flow while C for road capacity. α and β are experimental coefficients from realistic observation. These parameters can be obtained from the transportation network data package in the next section.

The energy cost E_{ij} for the EV is determined by a function of speed, travel distance, road conditions, and other factors. A simple example is when E_{ij} has a linear relationship with travel distance and the average speed, as shown in Equation (15).

$$E_{ij} = \gamma d_{ij} + \delta V, \forall i, j \in N \tag{15}$$

In this chapter, for the simplicity, we assume the EV will charge itself upon its arrival without waiting and the passengers are located at the pick-up nodes initially, which means the EV will start the trip from the pick-up nodes immediately.

2.3. Case Studies

Our case studies are developed based on the real-world transportation network, the city of Sioux Falls, South Dakota, as its data is readily accessible. Real-world survey and traffic flow data is used to generate required parameters for the proposed optimization problem [14].

The conventional Sioux Falls scenario presents static origin-destination matrices, and is transformed by Chakirov and Fourie [15], which is shown in Figure 2. Figure 3 represents the corresponding topology network, including 24 nodes and 76 edges.

Figure 2. Sioux Fall transportation system [15]

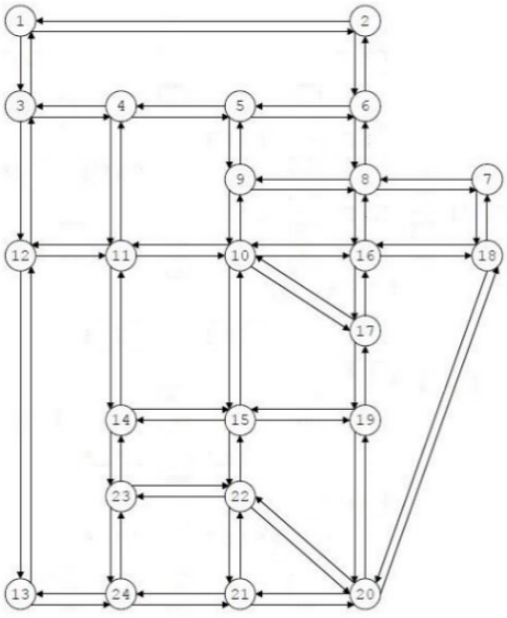

Figure 3. Simplified transportation network topology

2.3.1. The overall illustration of the optimal route

This scenario introduces the basic illustration of the optimal route on the network topology. Before searching the optimal route, we need to predefine some information about different types of nodes, including the start node, the end node, the pick-up nodes and the delivery nodes, as summarized in Table 1. The predefined charging stations are illustrated with yellow lightening figures and their locations are fixed. A randomly selected example is shown below.

Table 1: Nodes Clarification

Start node	End node	Pick-up nodes	Delivery nodes
3	17	5,10	14,22

Table 2: The Predefined SOC Requirements

Initial SOC	Boundaries for SOC
0.8	0.1—0.9

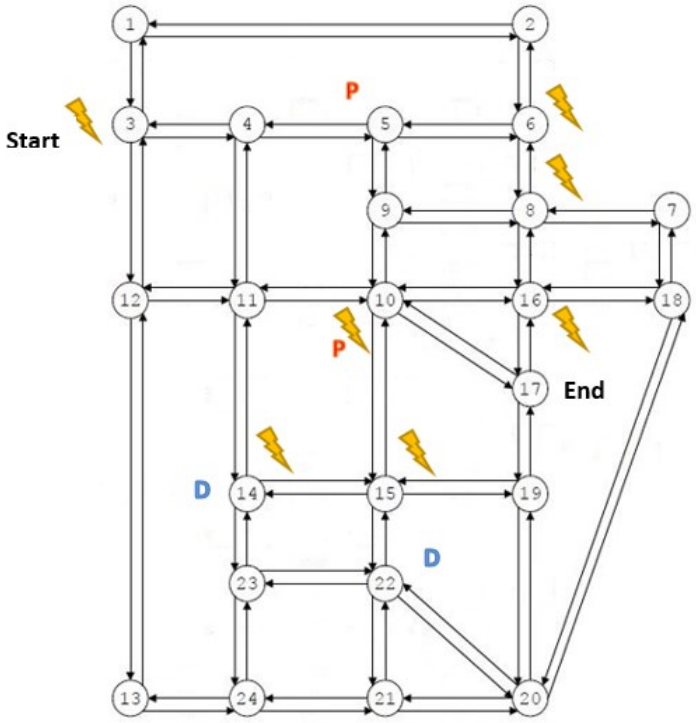

Figure 4. An illustration of different types of nodes

Table 2 presents the initial value and the limits for the EV SOC. Since there is only one single EV providing the service, we assume the maximum number of passengers is four and no overload problems exist.

2.3.2. The influence of different electricity prices

In this scenario, we set the EV as an Uber-like driver at a start node and pick up some customers at a certain nodes, then deliver them to their destination respectively. Meanwhile, the weighing terms are kept constant ($\omega_1, \omega_2, \omega_3$), which means passengers do not have special requirements on travel time or distance. The only factor that we consider is the price at the charging station (λ_i). All types of node information are summarized in Table 3, while the electricity prices at different charging stations are listed in Table 4.

Table 3: All Types of Nodes Clarification

Start node	End node	Pick-up nodes	Delivery nodes
9	7	5,10	14,22

Table 4: Two Sets of Charging Prices

Charging nodes	Charging Price beforehand ($/kWh)	Charging Price afterwards ($/kWh)
3	0.5	0.9
6	0.7	0.3
8	0.6	0.4
10	0.5	0.5
14	0.6	0.6
15	0.7	0.7
16	0.9	0.5

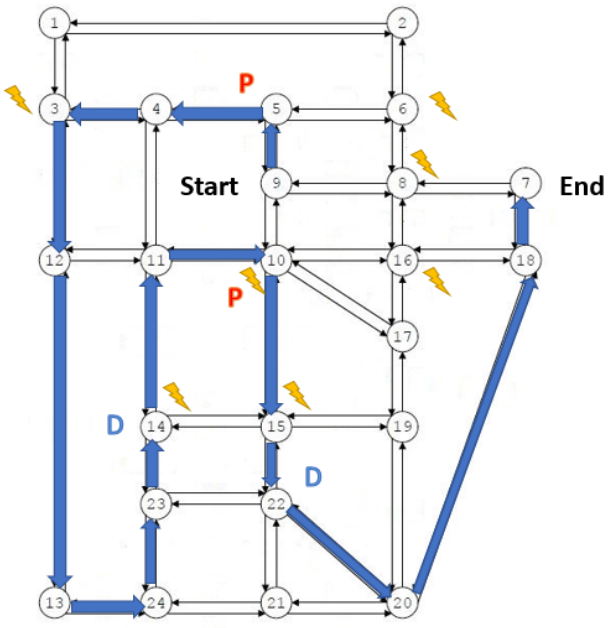

Figure 5. The optimal route for EV beforehand

In Figure 5, the ‘start’ and ‘end ’indicate the start node and the end node for the Uber-like EV, and the ‘P’ in red represents the pick-up nodes while the ‘D’ in blue indicates the delivery nodes. The yellow flashing labels represent charging stations located at certain nodes.

Given the dynamic electricity prices at various charging locations, the optimal route in Figure 6 is different from Figure 5. For example, the price at node 3 increases while the pierce at node 16 decreases. To save the charging cost, the EV’s optimal route changes from “9-8-6-5-4-3…” to “9-5-6-8-16…”. The abovementioned optimal routes indicate that the EV has stopped by more than one charging station.

The Table 5 summarizes the detailed information about the EV charging locations and the charging time. We can easily note that the EV obviously selected the charging station with less expensive prices such as node 6, 8 and 16 instead of node 3 and 10.

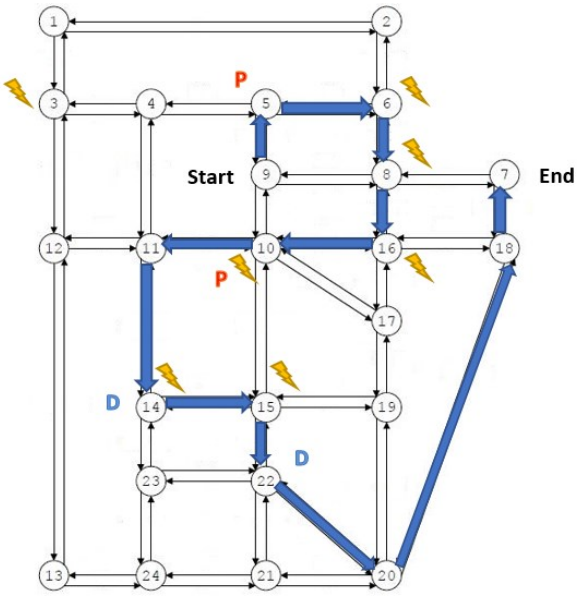

Figure 6. The optimal route for EV afterwards

Table 5: Charging Time at Different Stations

Charging nodes	Charging Time at first (min)	Charging Time after changing (min)
3	7	\
6	\	7.5
8	\	2.5
10	3.5	\
14	11	5
15	\	\
16	\	2

2.3.3. The preferences of different passengers

In this case, we consider the different passenger preferences and maintain the charging prices constant so that the EV driver can correspondingly make different route decision.

Passengers' preferences are presented by the change of weighing terms. For example, a passenger wants to save the total distance, which means he/she is not in a hurry and cares less about the travel time.

Basically, we consider two groups of passengers. The first group of passengers, as mentioned before, care less about the total travel time. For this preference, we can increase the weighing term of total travel distance (ω_1) and decrease the weighing of travel time (ω_2).

The other group of passengers are in urgent situations, which means the preference is travel time. For instance, they are about to be late for work, or have a flight to catch, etc. In those situations, arriving their destinations as soon as possible is the first priority. Correspondingly, we can increase ω_2 and decrease ω_1.

Figure 7 indicates the preference of saving distance while Figure 8 presents the preference of saving time. Apparently, the latter distance is much longer than the former one. That is consistent with the fact that there is a bigger chance for running into a traffic problem in the city-center instead of countryside. The second route is more likely a detour to save total travel time and meet the passenger's requirements.

It is important to note that although the electricity prices remain the same in this case, the EV driver's charging choices are different when changing ω_1 and ω_2 so that the SOC requirements and passenger preferences can be satisfied. Table 6 summarizes the charging time at different charging stations and Table 7 compares the total travel times for every passenger, where P_1 and P_2 represent two different passengers respectively.

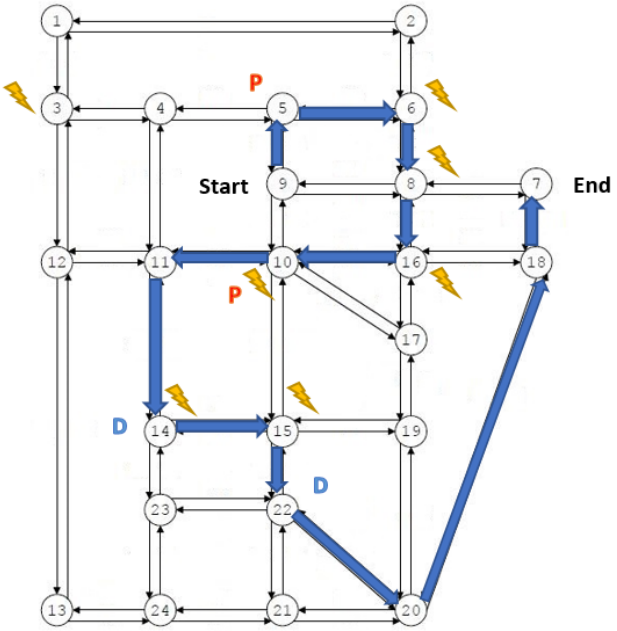

Figure 7. The optimal route with short travel distance

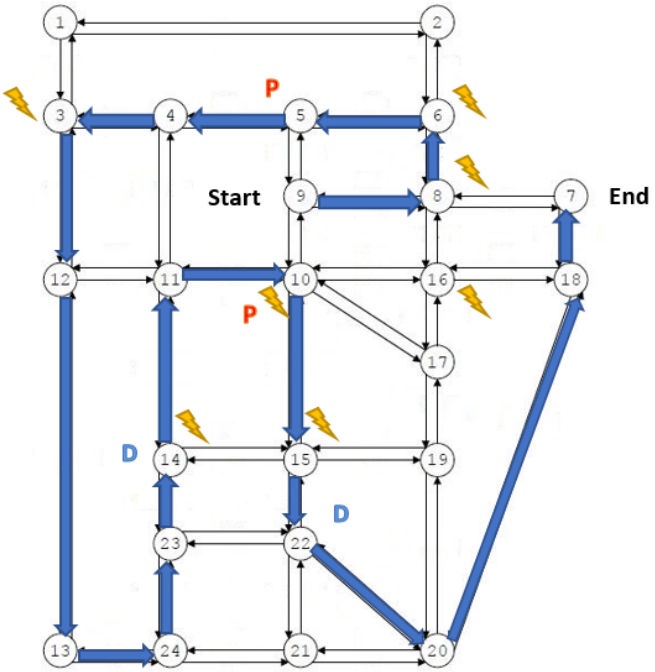

Figure 8. The optimal route for less travel time

Table 6: Charging Times at Different Nodes

Charging nodes	Charging Time when ω 1 increases (min)	Charging Time when ω 2 increases (min)
3	\	2.5
6	\	\
8	7.5	8
10	\	3.5
14	9.5	11
15	\	\
16	\	\

Table 7: Total Travel Time for Every Passenger

	Travel time for P_1 (min)	**Travel time for P_2 (min)**
When ω_1 increases	34.5	27.9
When ω_2 increases	26.9	12.5

2.4. Conclusion

In this chapter, we presented an optimal charging and routing problem of an Uber-like EV. Based on a real-world transportation network topology, three cases were developed. We considered the impact of electricity prices at different charging stations, and the impact of passengers' preferences. The proposed methodology facilitated the EV driver to determine the optimal routing and charging decisions in terms of charging cost, travel time and travel distance.

The proposed PDP-based optimization problem for a single EV can be extended to multiple EVs. Besides, the emerging Uber-like EVs will introduce a great amount of temporal-spatial uncertainties to power systems. There is an urgent need to develop sophisticated demand in response to more frequent charging requests.

2.5. References

[1] C. E. Cortés, M. Matamala, & C. Contardo (2010). The pickup and delivery problem with transfers: Formulation and a branch-and-cut solution method.*European Journal of Operational Research*, *200*(3), 711-724

[2] M. W. Savelsbergh, & M. Sol (1995). The general pickup and delivery problem. *Transportation science*, *29*(1), 17-29

[3] M. Buechel, J. Frtunikj, K. Becker, et al. "An automated electric vehicle prototype showing new trends in automotive architectures" 2015 IEEE 18th International Conference on Intelligent Transportaion Systems (ITSC), pp. 1274-1279, Sep.2015

[4] J. Moreno, M. E. Ortúzar, & J. W. Dixon, (2006). Energy-management system for a hybrid electric vehicle, using ultracapacitors and neural networks. *Industrial Electronics, IEEE Transactions on*, *53*(2), 614-623

[5] International Energy Agency, "Transport Energy and CO2: Moving Towards Sustainability", OECD Publishing, 2009

[6] J. Taylor, A. Maitra, M. Alexander, D. Brooks, & M. Duvall (2010, July). Evaluations of plug-in electric vehicle distribution system impacts. In *Power and Energy Society General Meeting, 2010 IEEE* (pp. 1-6)

[7] L. D. Burns (2013). Sustainable mobility: a vision of our transport future.*Nature*, *497*(7448), 181-182

[8] J. Xiong, K. Zhang, Y. Guo, and W. Su, "Investigate the Impacts of PEV Charging Facilities on Integrated Electric Distribution System and Electrified Transportation System", *IEEE Trans. on Transportation Electrification*, vol.1, no.2, pp.178-187, 2015

[9] W. Su, J. Wang, K. Zhang, and A.Q. Huang, "Model Predictive Control-based Power Dispatch for Distribution Systems Considering Plug-in Electric Vehicle Uncertainty", *Electric Power Systems Research*, vol.106, pp.29-35, January 2014

[10] N. Shi (2010). Constrained shortest path problem. *Automation Science and Engineering, IEEE Transactions on*, *7*(1), 15-23

[11] J. E. Beasley, & N. Christofides (1989). An algorithm for the resource constrained shortest path problem. *Networks*, *19*(4), 379-394

[12] Y. Guo, J. Xiong, S. Xu, and W. Su, "Two-Stage Economic Operation of Microgrid-like Electric Vehicle Parking Deck", *IEEE Trans. on Smart Grid*, 2015

[13] N. He, and S.Zhao, "Discussion on Influencing Factors of Flee-flow Travel Time in Road Traffic Impedance Function", Procedia-Social and Behavioral Sciences, Vol.96, pp. 90-97, 2013

[14] T. L. Friesz, H. J. Cho, N. J. Mehta, R. L. Tobin, & G. Anandalingam (1992). A simulated annealing approach to the network design problem with variational inequality constraints. *Transportation Science*, *26*(1), 18-26

[15] A. Chakirov, and P. Fourie. *Enriched sioux falls scenario with dynamic and disaggregate demand*. Working paper, Future Cities Laboratory, Singapore-ETH Centre (SEC), Singapore, 2014

Chapter 3

Distance-based Long Term Optimization and Power Management for Power-split Hybrid Electric Vehicle

Nomenclature

$m_f(k)$	Vehicle fuel rate at location k
$v(k)$	Vehicle speed at location k (m/s)
$v_{ref}(k)$	Reference speed at location k (m/s)
$v'(k)$	Vehicle acceleration at location k (m/s^2)
$\omega_e(k)$	Engine speed at location k (rad/s)
$\omega_{motor}(k)$	Motor speed at location k (rad/s)
$\omega_{ring}(k)$	Ring gear speed at location k (rad/s)
$\omega_{gen}(k)$	Generator speed at location k (rad/s)
$T_e(k)$	Engine torque at location k (Nm)
$T_{motor}(k)$	Motor torque at location k (Nm)
$T_{ring}(k)$	Ring gear torque at location k (Nm)
$T_{gen}(k)$	Generator torque at location k (Nm)
$T_{demand}(k)$	Vehicle demand torque at location k (Nm)
$P_e(k)$	Engine power at location k (kW)
$P_{motor}(k)$	Motor power at location k (kW)
$P_{ring}(k)$	Ring gear power at location k (kW)
$P_{batt}(k)$	Battery power at location k (kW)

$P_{gen}(k)$	Generator power at location k (kW)
$P_{demand}(k)$	Vehicle demand power at location k (kW)
$F_{brake}(k)$	Brake force at location k (Nm)
$t(k)$	Driving time at location k (s)
Δt_k	Time interval between location k and $(k+1)$ (s)
$I_{batt}(k)$	Battery current at location k (A)
$SOC(k)$	Battery state-of-charge (SOC) at location k
P_l	Vehicle electrical load power (kW)
Δs	Distance interval (m)
N	Number of locations in the driving cycle
ω_1	Weighing term for vehicle fuel rate
ω_2	Weighing term for vehicle speed deviation
α	Constant in fuel rate model
β	Constant in fuel rate model
N_r	Number of teeth of the ring gear
N_s	Number of teeth of the sun gear
λ	Ratio of teeth between ring and sun gear
R_{wheel}	Radius of the vehicle wheels (m)
m	Mass of the vehicle (kg)
ρ	Air density (kg/m^3)
C_d	Drag coefficient
A_d	Front area of the vehicle (m^2)
g	Gravity (m/s^2)

C_r	Rolling resistance coefficient
θ	Road gradient (rad)
γ_{final}	Final drive ratio
V_{oc}	Open circuit voltage (V)
R	Battery internal resistance (Ω)
Q_{max}	Maximum battery capacity (Ah)
n_{pop}	Number of populations
n_{iter}	Number of iterations
t_r	Population truncation ratio
J_{EDA}	Final cost value generated by EDA method
J_{GA}	Final cost value generated by GA method

3.1. Introduction

Due to the growing energy requirement and environmental concerns, the development of vehicles with less emissions and high fuel efficiency has become a popular research trend in the automobile industry. Hybrid Electric Vehicles (HEVs) have emerged as a promising advanced technology to improve fuel economy while satisfying the tightened emission standards [1]. By applying a secondary power source, HEVs offer a significant improvement in fuel economy compared with vehicles with the traditional drivetrain [2].

Based on the powertrain system design, the HEV models can be divided into three categories: parallel hybrid, series hybrid and power-split hybrid [3]. Because power-split HEVs have more energy flow paths and operating modes compared to other configurations, the management of energy cost and driving pattern becomes more complicated.

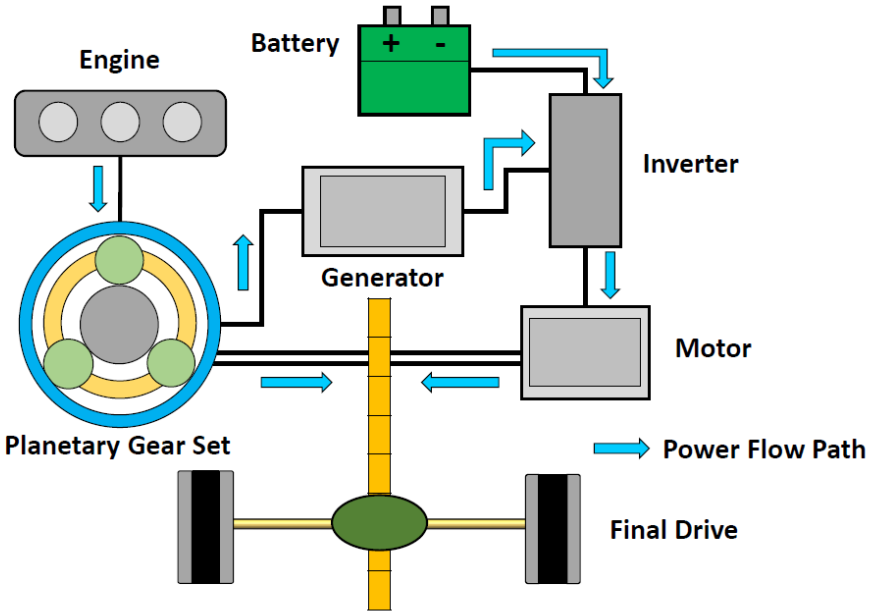

Figure 9. Power-split HEV powertrain configuration

The power-split mechanisms were studied as early as the 1970s [4]. The Toyota Hybrid System (THS), the core of the first commercial power-split HEV offered in 1997 in Japan, the Toyota Prius, was described in [5]. Figure 9 illustrates the power-split HEV powertrain configuration. It combines the parallel and series hybrid designs. On one hand, similar to the parallel hybrid design, it has the separate engine power-flow path and battery-motor power-flow path. Instead of transmission, it implements a power-split planetary gear set, to link the engine with the final drive. On the other hand, similar to the series hybrid design, it has the engine-generator power-flow path. The engine drives a generator to either charge the battery or supply power to the motor.

Figure 10 shows the power flow in a power-split HEV configuration. The output power from the engine can be split into the power at ring gear and the power at generator. The ring gear power represents the mechanical power flow path from the engine to the ring gear to the final drive. The generator power represents the electrical path from the engine to the motor to the final drive. The split of the engine output power between the mechanical path and the electrical path is accomplished by controlling the engine speed with the generator. The two

power paths provide propulsion power to the final drive to simultaneously or independently move the vehicle forward [8].

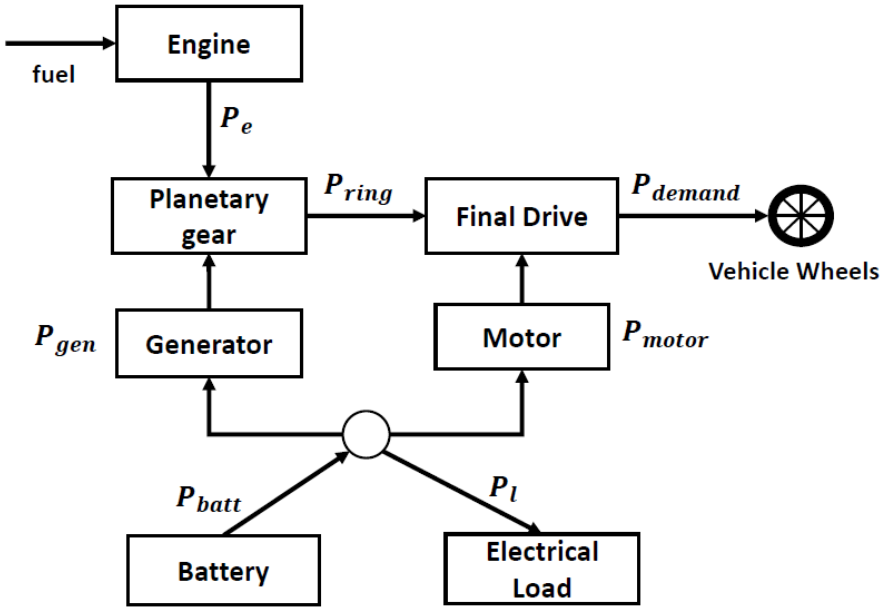

Figure 10. Power flow in a power split HEV configuration

Existing HEV power management approaches are mostly based on a time domain. Dynamic Programming (DP) is widely implemented as an optimization method since this algorithm can solve the global optimization problem of a nonlinear objective function with various constraints [9]. Other approaches, for example, the Model Predictive Control (MPC) is usually employed. But its final optimization results are largely dependent on the horizon length [10]. While a long horizon with reliable prediction data improves the vehicle fuel economy, it still requires much computing time. There is little work that addresses the HEV power management in the distance domain, while considering constraints from different perspectives.

This chapter addresses the long term optimization under a test driving cycle for an individual HEV, by utilizing the estimation of distribution algorithm (EDA) methods. The objective function mainly consists of vehicle fuel consumption and vehicle speed deviation. Constraints from the HEV powertrain model, road conditions, and speed limits are considered.

The major contributions of this chapter are as follows:

(1) Develop a mathematical power-split HEV powertrain model for achieving a vehicle fuel efficiency improvement and optimizing the vehicle speed over a driving cycle;

(2) Under the distance domain, generate not only the vehicle optimal speed, but also vehicle battery state-of-charge (SOC) information for each distance step;

(3) Utilize the EDA method for solving nonlinear and constrained complex objective function, to demonstrate the feasibility, accuracy, robustness, and effectiveness of the proposed HEV model.

The remainder of this chapter is organized as follows. Section II will describe the system mathematical formulation. The objective function and system constraints will be provided. Section III will review the EDA method, as well as describe how this algorithm implements for the proposed optimization problem. The results and analysis of the simulation are presented in Section IV. Finally, Section V will summarize this chapter.

3.2. Problem Formulation

The proposed Long term optimization is conducted before the HEV departure. Figure 11 illustrates a driving route example for the proposed distance-based long term optimization system. In the distance domain, the entire route is divided into several segments. The driving time from departure to the destination is estimated. An expected optimal speed profile, also the vehicle SOC information for all locations are generated, by using characteristics of the power-split HEV powertrain, driver-oriented data (e.g., final destination, recent trip information, driver's own preference) and standard data (e.g., GPS data, weather conditions, road conditions, the speed limits).

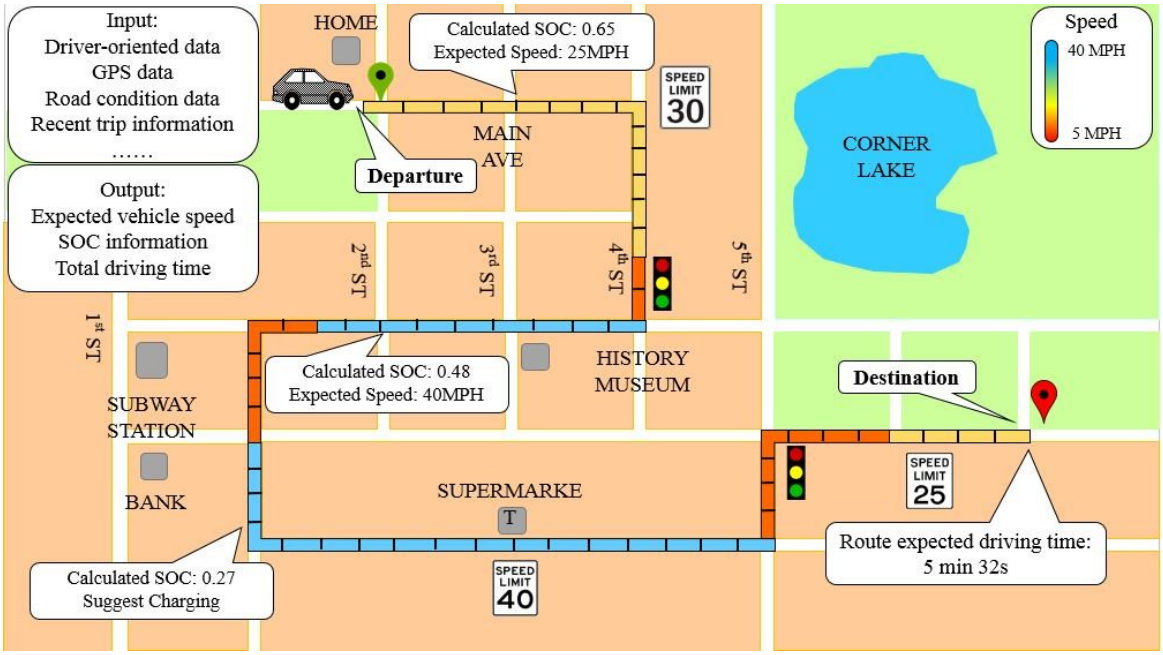

Figure 11. A Driving Route Example for the Distance-based Long Term Optimization System

In the time domain, any adaptation of the speed profile due to traffic conditions or speed limits, changes the total driving time. And all the speed values after that time changes with it, even if the adjusted time period is very short compared to the entire driving time. Consequently, the remaining speed profile is required to be computed again. Moreover, since the traffic conditions change frequently, the speed profile is calculated back and forth, and the entire computational time for the optimization turns out extremely long, which is not desirable for ecological driving [11].

However, in a distance-based driving cycle, when a speed adaptation happens, only the speeds of surrounding segments which are directly affected by traffic conditions are changed and for the remaining route, the original speed profile can maintain effective. For example, as long as the heavy traffic regions are not too wide, and few traffic signals in the driving route, the computational cost for every speed adaptation is small and the long-term optimization can be maintained. This explains the reason for conducting the pre-trip optimization in the distance domain.

3.3. Objective Function

The objective function being considered in this optimization system is the minimization of J. As shown in equation (1), the objective function consists of two terms. The first term mainly minimizes the HEV fuel cost, the m_f stands for the vehicle fuel rate, and Δt_k represents the time difference, which is expressed in (4), and the second term concerns the vehicle speed deviation. It intends to make the actual vehicle speed as close as possible to the target speed v_{ref}. Figure 12 illustrates an example of the target speed profile in the distance domain, the entire driving cycle in this optimization is divided into $(N+1)$ locations, with the identical distance of Δs. Consequently, the total distance of the driving cycle is $N\Delta s$. ω_1 and ω_2 are weighing factors for each term.

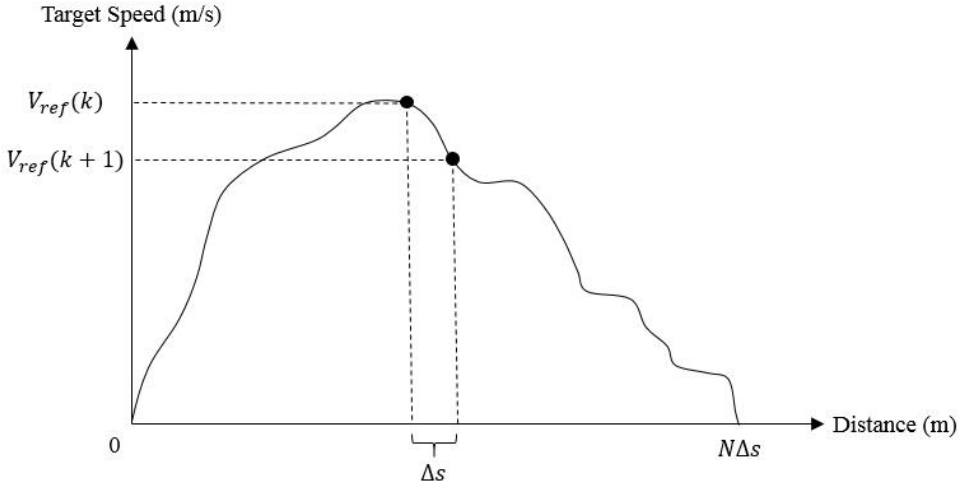

Figure 12. Target Speed profile in the distance domain

$$\min J = \alpha_1 \sum_{k=1}^{N} m_f(k)\Delta t_k + \alpha_2 \sum_{k=1}^{N} \left[v_{ref}(k) - v(k)\right]^2 \quad (1)$$

$$m_f = (\alpha_1 \omega_e(k) + \alpha_2) T_e(k) + \beta_1 \omega_e(k) + \beta_2 \quad (2)$$

$$T_e(k) = f[\omega_e(k), P_{batt}(k), F_{brake}(k), v(k-1), v(k)] \quad (3)$$

$$\Delta t(k) = t(k+1) - t(k) = \frac{2\Delta s}{V(k)+V(k+1)} \quad (4)$$

The engine speed ω_e, the vehicle battery power P_{batt}, the brake force F_{brake}, and the

vehicle speed v are considered as the inputs. Based on Willans Line approximation method [13], the vehicle fuel rate m_f can be expressed by the engine rotational speed ω_e, and the engine torque T_e, as shown in equation (2), where α_1, α_2, β_1 and β_2 are constants. Furthermore, equation (3) shows that the engine torque T_e is a function of those four variables. The detailed expression of T_e is derived by the following procedure.

Equation (5) and (6) describe the torque relationship inside the HEV powertrain model. T_e can be either expressed by the ring gear torque T_{ring}, or the vehicle generator torque T_{gen}. N_r and N_s are the number of teeth of the ring and sun gear. To simplify the formulation, λ represents the teeth ratio between the sun gear and the ring gear.

$$T_e(k) = \frac{N_r + N_s}{N_r} T_{ring}(k) = (1 + \lambda) T_{ring}(k) \tag{5}$$

$$T_e(k) = \frac{N_r + N_s}{N_s} T_{gen}(k) = \left(1 + \frac{1}{\lambda}\right) T_{gen}(k) \tag{6}$$

$$T_{demand}(k) = T_{ring}(k) + T_{motor}(k) = \frac{1}{1 + \lambda} T_e(k) + T_{motor}(k) \tag{7}$$

From Figure 9, we find that both the ring gear and the vehicle motor are connected to the final drive line, which means the final torque demand of the vehicle consists of the ring gear torque T_{ring} and the motor torque T_{motor}. Thus, the equation (7) can be obtained. Also, to denote T_e, the expressions for T_{demand} and T_{motor} should be obtained first.

In order to derive another equation of the final torque demand T_{demand}, the vehicle dynamic equation (8) is applied, where $C_1 = \frac{1}{R_{wheel}}$, $C_2 = \frac{1}{2}\rho C_d A_d$, and $C_3 = mgC_r cos\theta + mgsin\theta$. R_{wheel} is the radius of the vehicle wheels and $m, \rho, C_d, A_d, g, C_r$ and θ are the mass of the vehicle, the air density, the drag coefficient, the frontal area of the vehicle, the gravity, the rolling resistance coefficient, and the road gradient, in order. All these parameters are modeled with the data obtained from Autonomie, a software for simulating performance of different types of vehicles, designed by Argonne National Laboratory [14]. The values of

parameters in equation (8) are listed in Table 8. Also, in order to express the vehicle acceleration $v'(k)$, equation (9) and (10) are applied.

Table 8: Constant Parameter Values

Parameters	**Values**
m	1607 kg
R_{wheel}	0.30115 m
ρ	1.19854 kg/m^3
C_d	0.3
A_d	2.25084 m^2
g	9.81 m/s^2

$$T_{demand}(k) = \frac{mv'(k) + C_2 v(k)^2 + C_3 + F_{brake}(k)}{C_1} \tag{8}$$

$$\mathrm{v(k+1)} = \mathrm{v(k)} + v'(k)\Delta t_k \tag{9}$$

$$v'(k) = \frac{v(k+1) - v(k)}{\Delta t_k} = \frac{v(k+1)^2 - v(k)^2}{2\Delta s} \tag{10}$$

To express the vehicle motor torque T_{motor}, equations from (11) to (15) are implemented. From Figure 10, we find that one of the vehicle power flow equations can be expressed by (11), where P_{motor} and P_{gen} represents the motor power and generator power, respectively. P_l denotes the electrical load and is kept constant. Equation (12) describes the relationship between vehicle motor speed ω_{motor} and ring gear speed ω_{ring}, where γ_{final} represents the final drive ratio and it is kept as a constant. Equation (13) presents the relationship among the generator speed ω_{gen}, the engine speed ω_e and the motor speed ω_{motor}. Combine the equations from (11) to (14), the vehicle motor torque T_{motor} can be derived in (15).

$$P_{motor}(k) = P_{batt}(k) + P_{gen}(k) - P_l \tag{11}$$

$$\omega_{motor}(k) = \omega_{ring}(k) = \frac{V(k)}{R_{wheel}} \times \gamma_{final} \tag{12}$$

$$\omega_{gen}(k) = \left(1 + \frac{1}{\lambda}\right)\omega_e(k) - \frac{1}{\lambda}\omega_{motor}(k) \tag{13}$$

$$P_{gen}(k) = T_{gen}(k)\omega_{gen}(k) \tag{14}$$

$$T_{motor}(k) = \frac{P_{motor}(k)}{\omega_{motor}(k)}$$

$$= \frac{\left[P_{batt}(k) + (T_e(k)\omega_e(k) + \frac{T_e(k)\gamma_{final}}{(\lambda+1)R_{wheel}}v(k)) - P_l\right]R_{wheel}}{v(k)\gamma_{final}} \quad (15)$$

Since the expression of T_{demand} and T_{motor} are all derived, the engine torque T_e can be calculated and the detailed expression (16) is expressed below. Furthermore, the HEV fuel rate m_f can be calculated by those four control inputs.

$$T_e(k)$$

$$= \frac{\frac{1+\lambda}{C_1}\left[m\frac{v(k+1)^2 - v(k)^2}{2\Delta s} + C_2 v(k)^2 + C_3 + F_{brake}(k)\right] - \frac{(1+\lambda)R_{wheel}}{v(k)}(P_{batt}(k) - P_l)}{2\gamma_{final} - \frac{(1+\lambda)R_{wheel}\omega_e(k)}{v(k)}} \quad (16)$$

For the second term in the final objective function, the reference speed v_{ref} is given based on the speed limit, or the average speed of every distance step. As shown in Figure 13, the applied target speed profile of the entire driving cycle is presented.

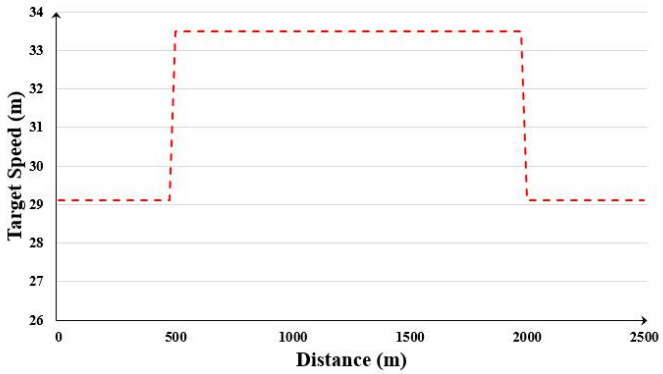

Figure 13. Pre-trip target speed profile

3.4. System Constraints

Both equality and inequality constraints of each distance step are considered in this chapter. For inequality constraints, four control variables ($\omega_e, P_{batt}, F_{brake}$ and v) have upper and lower bounds, as shown from equation (17) to (20). In terms of each component in the power-

split HEV powertrain model, its physical, and vehicle dynamic constraints are considered. For example, in equation (12), the rotational speed limits for ω_{motor} are considered and they update the limits for $v(k)$.

$$\omega_{e\_min}(k) \leq \omega_e(k) \leq \omega_{e\_max}(k) \tag{17}$$

$$P_{batt\_min}(k) \leq P_{batt}(k) \leq P_{batt\_max}(k) \tag{18}$$

$$F_{brake\_min}(k) \leq F_{brake}(k) \leq F_{brake\_max}(k) \tag{19}$$

$$v_{min}(k) \leq v(k) \leq v_{max}(k) \tag{20}$$

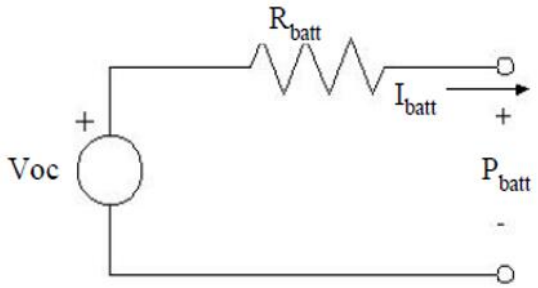

Figure 14. The HEV battery equivalent circuit

The vehicle battery constraints are also included. As shown in Figure 14, an equivalent circuit with an internal resistance R, is implemented as the HEV battery model, where V_{oc} stands for the open circuit voltage, and I_{batt} represents the battery current. The battery temperature is assumed to be constant and the temperature effect is ignored. From the equivalent circuit, equation (21) can be derived.

$$I_{batt}(k) = \frac{-V_{oc} + \sqrt{V_{oc}^2 - 4[P_{batt}(k)R]}}{2R} \tag{21}$$

$$I_{batt\_min}(k) \leq I_{batt}(k) \leq I_{batt\_max}(k) \tag{22}$$

The vehicle battery SOC represents the electrical status of the battery. The battery current are limited in equation (22) and the initial SOC is pre-set. The SOC expression for following distance steps is presented in equation (23), where Q_{max} represents the maximum battery capacity and it is kept as a constant of 1.6kWh during the whole optimization. As shown in (24), for every distance step, the SOC should satisfy its limits, which are 0.2 and 0.8 for the

minimum and maximum value, respectively.

$$SOC(k+1) = SOC(k) + \frac{I_{batt}(k)\Delta t_k}{Q_{max}} \tag{23}$$

$$SOC_{min}(k) \leq SOC(k) \leq SOC_{max}(k) \tag{24}$$

For equality constraints, as shown in Figure 10, the power-split HEV power flow equations, such as equation (11), should be satisfied during the entire driving cycle.

3.5. EDA Application

In this chapter, the system final objective function is a nonlinear and complicated function with the control inputs of $\omega_e, P_{batt}, F_{brake}$ and v. EDA is implemented for solving this pre-trip optimization problem. To compare the simulation results and demonstrate the feasibility, accuracy, robustness, and effectiveness of the proposed model, the genetic algorithm (GA) is also utilized and its results are set to be the benchmark. Both two algorithms can optimize this problem while considering constraints from various perspectives.

EDAs are evolutionary algorithms based on global statistical information extracted from promising solutions [17]. It is a stochastic optimization methods which build a probability distribution from the promising populations by using the probability distribution model. The probability-based generation of samples in an EDA can speed up the optimization and provide an explicit structure to the problem.

For the pre-trip optimization problem, some details are as follows.

1) Initially generate a predefined number of samples of all control inputs for N locations. In this simulation, the total number of populations is n_{pop}, and each population consists of N pairs of $\omega_e, P_{batt}, F_{brake}$ and v.
2) Values of the objective function for all initial samples are calculated and compared. Since this is a minimization problem, those samples with smaller values are selected. The

number of chosen samples is given by the multiplication of the number of populations and the truncation ratio, $n_{pop} \cdot t_r$.

3) The probability distributions, such as the average and the standard deviation of the selected samples are calculated.

4) Randomly generate $n_{pop} \cdot (1 - t_r)$ new solutions subjected to all constraints, based on the normal distribution with the calculated average and standard deviation.

5) Replace some samples from the current population with the offspring generated.

6) Repeat the steps from 2 to 5 until the maximum number of iterations, or the minimum error criteria is met. And save the near-optimal solution.

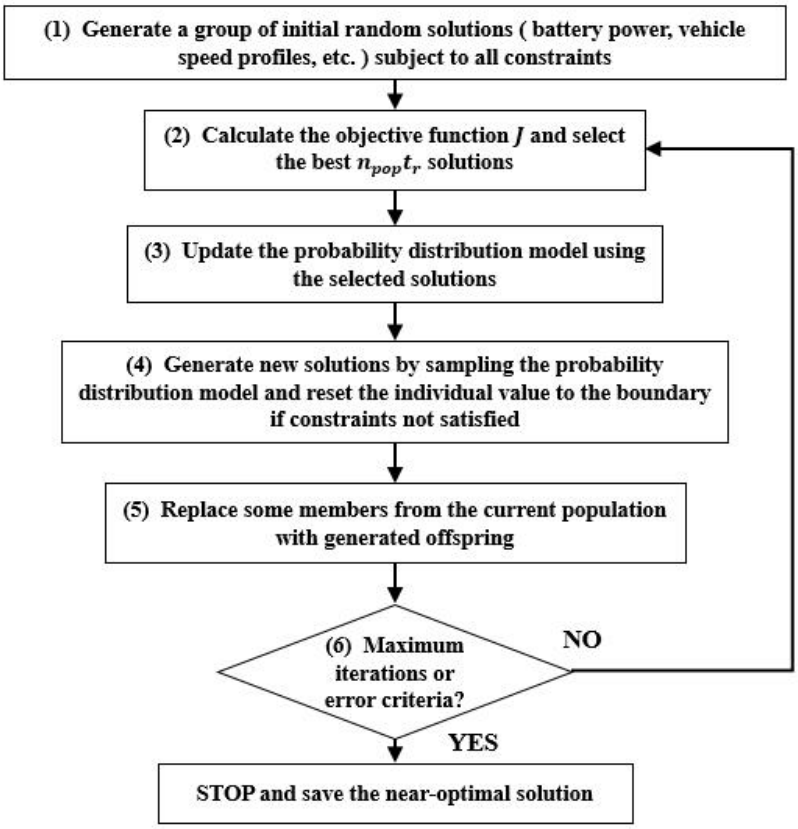

Figure 15. The flowchart of EDA

For the EDA initial population, they are generated under normal distribution. Since the characteristics of the entire system are unknown, new optimal ranges of the control inputs are estimated by the average and standard deviation of the previous population set.

Although the pre-trip optimization is performed before the HEV departure, the

computational time should not be too long. The following approaches are implemented for shortening the computing time. First, the initial populations are generated by the estimated possible solution area instead of random generation. Due to the physical limits and general information from the HEV drivetrain, the possible area can be estimated. For example, the average values of the control inputs in the initial population are simply assumed by the linear vehicle acceleration and deceleration in speed transition regions. Second, a small truncation ratio is adopted with large populations, by taking the relationship between t_r and n_{op}. More exchange can happen by using a small t_r and consequently may bring a faster convergence. In this pre-trip problem, the t_r is set to be 0.3 while the n_{pop} is 400.

The EDA is selected for solving this problem because it is robust for nonlinear and complex optimization problems with few parameters to control. Besides, the EDA performance is not largely affected by the size of the problem, or the computer memory limits. Compared with other approaches, EDA can maintain a low computational cost without modifying too much system parameters.

While the original objective function can be minimized by GA, its computational time is much longer than of the same objective function by EDA, and thus, it is only used as a benchmark.

3.6. Simulation and Analysis

All proposed Long Term simulations are run on an Intel(R) Core(TM) i7-4712HQ CPU @ 2.30GHz, 16.0GB, Windows 8, and solved by Matlab 2016b. As introduced in the previous section, the EDA is utilized to optimize the final cost function. To test the validity of the proposed framework, the GA method is also implemented.

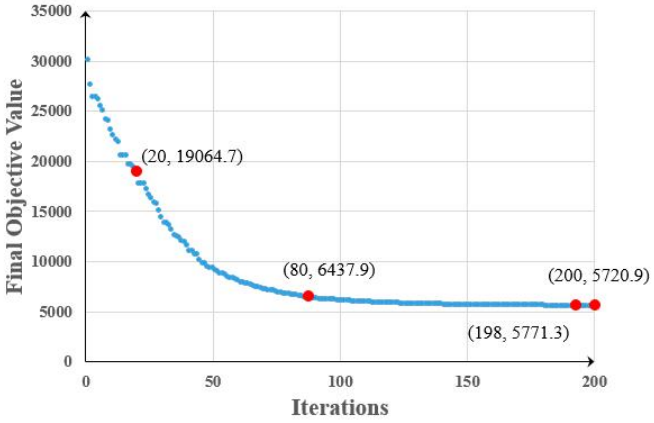

Figure 16. Convergence tendency of the EDA method

The typical convergence procedure of the EDA is presented in Figure 16. The maximum number of iterations n_{iter} is set to be 200. The population size in solving this optimization problem is set as 400. The blue dotted line represents the final fitness value. Eventually, it converges with the optimal value of 5720.9 at the 200th iteration. This result shows the proposed method is capable of obtaining good quality solutions with stable convergence characteristic.

When the second weighing term ω_2 is smaller than 1, the final vehicle speed is lower than the target speed by more than 10%, which is not a balanced driving. Therefore, only ω_2 is equal or larger than 1 are considered. In this simulation, ω_2 is set to be 2, and in order to balance two terms in the objective function, ω_1 is set to be 10^5.The final speed of the entire driving cycle should be zero. This is implemented by adding another term of $\omega_3(v(N+1)-0)$ into the function and set ω_3 to be 10^8.

To test the validity of the proposed power-split HEV model by EDA, the driving route under test is 2.5 kilometers long and the distance step Δs is set to be 25m. Consequently, the number of distance step is 101. For the entire route, the road gradients are assumed to be zero.

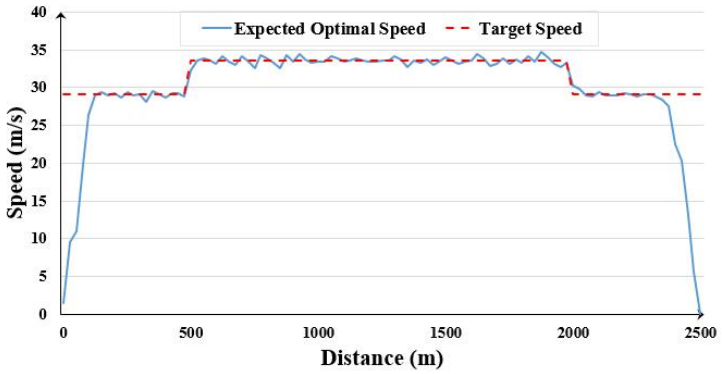

Figure 17. Final Speed Profile of EDA method

Figure 17 shows the optimal speed profile generated for the test route. The solid blue line represents the optimal speeds and the dotted line represents the speed limits, which are used as target speeds. Despite the start and end of the route, which indicate the acceleration and deceleration of the vehicle, the final speed generally follows the target speed profile. Figure 18 presents the vehicle SOC for the entire test route. The initial SOC is set to be 0.6 and SOC in every distance step is maintained within the limited range, which is 0.2 to 0.8.

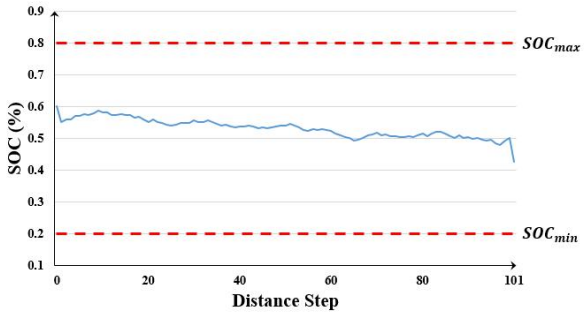

Figure 18. Vehicle SOC of EDA method

The histograms in Figure 19, 20 and 21 show the simulation results by EDA and GA, which are vehicle fuel consumption, total driving time difference, and the computational time for the entire test route, respectively. For both methods, 30 trials are conducted. It is important to mention that the 30 trials are performed randomly and subject to all system conditions and constraints.

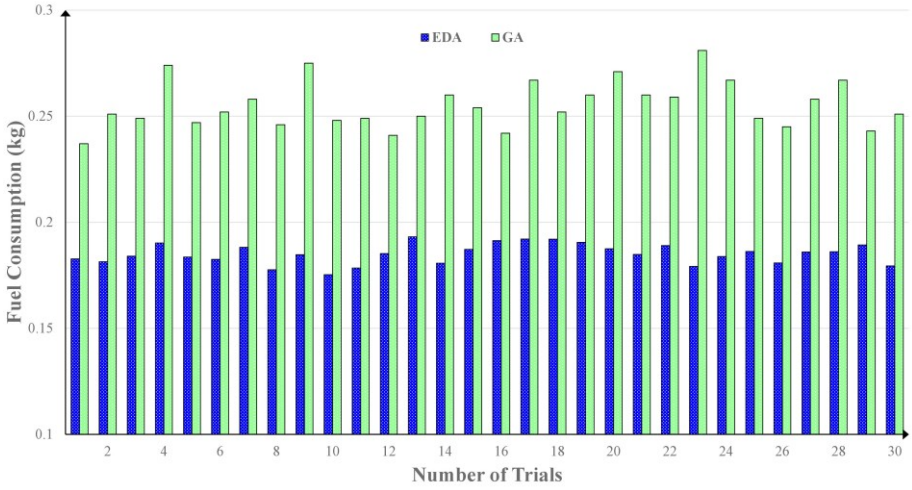

Figure 19. EDA and GA Fuel Consumption Comparison

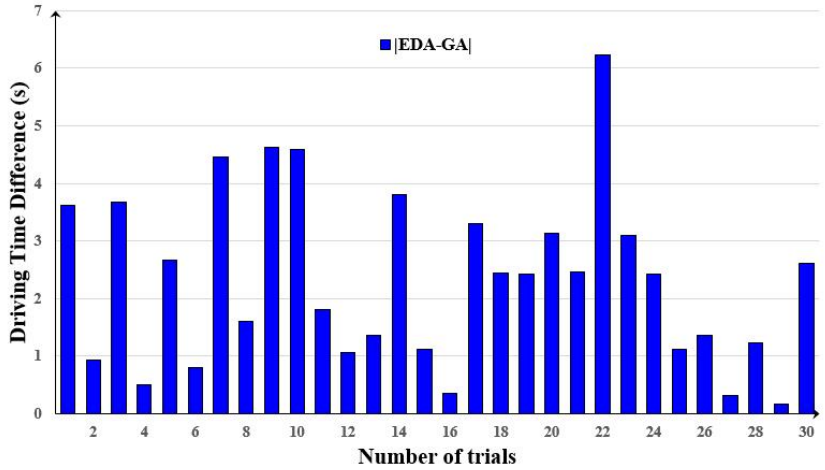

Figure 20. EDA and GA Total Driving Time Comparison

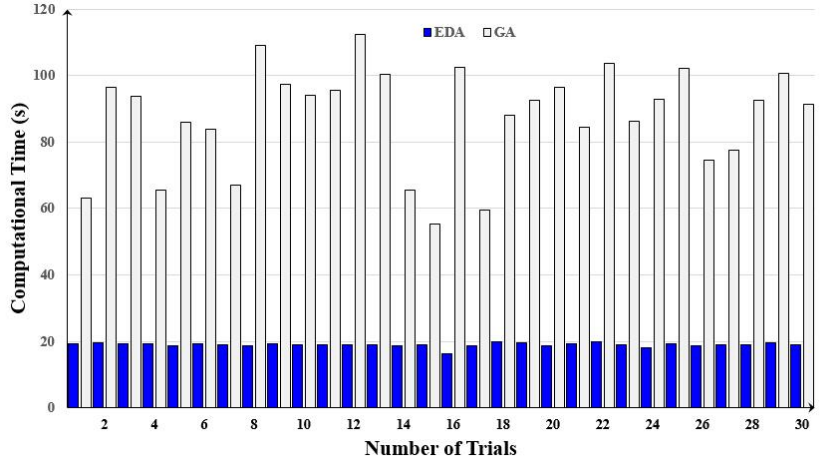

Figure 21. EDA and GA Computational Time Comparison

The EDA results are compared with the results generated by GA. In EDA, the average

estimated fuel consumption is 0.185 kg, the average total driving time is 111.01 seconds, and the average computational time is 19.00 seconds for this long-term optimization, while in GA, those values are 0.255kg, 112.79 seconds, and 87.73 seconds, respectively.. Table 9 describes the average final cost values generated from EDA and GA. The standard deviations of final cost values of EDA and GA are 2.6% and 3.1%, respectively.

Table 9: Comparison on EDA and GA with 30 Trials

	Final Cost Value	**Standard Deviation**
EDA	5720.9	147.6
GA	7730.6	235.9

In comparing the EDA results with the GA results, the average total driving times are almost the same in the range from 0 to 4%, but the average fuel consumptions computed by EDA are better than those produced by GA by 26%. They have a wider distribution in GA. The maximum fuel consumption in EDA is smaller than the value calculated by the GA method. In particular, EDA is less time-consuming than GA because selection and crossover functions are not required in EDA method. Besides, most parameters need to be tuned by users. So the parameter setting is a huge factor that influences the GA performance. Instead, EDA can generate new offspring from its previous iteration result.

To compare the system optimization performance, the equation is defined as:

$$System_{Performance} = \left| \frac{\bar{J}_{EDA} - \bar{J}_{GA}}{\bar{J}_{GA}} \right| \times 100\% \tag{25}$$

$\bar{J}_{EDA}$ and $\bar{J}_{GA}$ are the average final cost values generated from EDA and GA, respectively. Therefore, based on the information provided from Table 9, we can conclude that the EDA method improves the system performance by 25.0%, and thus, the long-term optimization by EDA is sufficiently competitive for ecological driving.

3.7. Conclusion

In this chapter, we described the distance-based pre-trip optimization for the power-split HEV by implementing GA and EDA methods. The vehicle powertrain model was

mathematically constructed. In order to optimize the final objective function which consists of the vehicle fuel cost and also the speed deviation, and constrained by the vehicle powertrain limits, the traffic conditions, and speed limits, both GA and EDA methods were utilized and the simulation results generated by GA was set to be the benchmark for EDA results. Both results demonstrated the feasibility, accuracy, robustness, and effectiveness of the proposed power-split HEV model. In addition, the proposed vehicle model can be tailored and extended with real-time implementation in the near future.

3.8. References

[1] M. Koot, J. T. Kessels, B. De Jager, Heemels, W. P. M. H., J. P. P. Van den Bosch, & M. Steinbuch, "Energy management strategies for vehicular electric power systems". *IEEE transactions on vehicular technology*, *54*(3), 771-782, 2005

[2] Johnson, H. Valerie, B. Wipke Keith, and J. Rausen David. "*HEV control strategy for real-time optimization of fuel economy and emissions"*. No. 2000-01-1543. SAE Technical Paper, 2000

[3] B. M. Baumann, G. Washington, B. C. Glenn, and G. Rizzoni, "Mechatronic design and control of hybrid electric vehicles," *IEEE/ASME Trans. Mechatron.*, vol. 5, no. 1, pp. 58–72, Mar. 2000

[4] L. Guzzella and A. Sciarretta, *Vehicle Propulsion Systems—Introduction to Modeling and Optimization*. Berlin, Germany: Springer-Verlag, 2005

[5] J. Liu, & H. Peng, "Modeling and control of a power-split hybrid vehicle". *IEEE transactions on control systems technology*, *16*(6), 1242-1251, 2008

[6] W. Li, A. Abel, K. Todtermuschke, & T. Zhang. "Hybrid vehicle power transmission modeling and simulation with simulation X". In *Mechatronics and Automation, 2007. ICMA 2007. International Conference on* (pp. 1710-1717). IEEE, 2007

[7] H.S. Yu, J. W. Zhang, & T. Zhang. "Control strategy design and experimental research on a four-shaft electronic continuously variable transmission hybrid electric vehicle". *Proceedings of the Institution of Mechanical Engineers, Part D: Journal of Automobile Engineering*, *226*(12), 1594-1612, 2012

[8] Y. L. Murphey, J. Park, Z. Chen, M.L. Kuang, M.A. Masrur, & A.M. Phillips, (2012). "Intelligent hybrid vehicle power control—Part I: Machine learning of optimal vehicle power". *IEEE Transactions on Vehicular Technology*, *61*(8), 3519-3530

[9] H. Borhan, A. Vahidi, A.M. Phillips, M.L. Kuang, I.V. Kolmanovsky, & S. Di Cairano. "MPC-based energy management of a power-split hybrid electric vehicle". *IEEE Transactions on Control Systems Technology*, *20*(3), 593-603, 2012

[10] W. Su, and M.-Y. Chow, "Performance Evaluation of A PHEV Parking Station Using Particle Swarm Optimization", *2011 IEEE Power and Energy Society General Meeting*, Detroit, Michigan, U.S.A. July 24-29, 2011

[11] H. Lim, W. Su, and C. C. Mi, "Distance-based ecological driving scheme using a two-stage hierarchy for long-term optimization and short-term adaptation," *IEEE Transactions on Vehicular Technology*, to be published

[12] H. Lim, W. Su, and C. Mi, "Distance-based Ecological Driving Scheme using a Two-stage Hierarchy for Long-term Optimization and Short-term Adaptation", *IEEE Trans. on Vehicular Technology*, 2016

[13] M. Duoba, H. Lohse-Busch, R. Carlson, T. Bohn, & S. Gurski. "*Analysis of power-split HEV control strategies using data from several vehicles"* (No. 2007-01-0291). SAE Technical Paper, 2007

[14] Argonne National Laboratory, AUTONOMIE, [Online]. http://www.autonomie.net

[15] N. Kim, A. Rousseau, and E. Rask, "Autonomie model validation with test data for 2010 Toyota Prius," in *Proc. SAE*, Detroit, MI, USA, 2012, pp. 1-14

[16] N. Kim, M. Duoba, N. Kim, and A. Rousseau, "Validating Volt PHEV model with dynamometer test data using Autonomie," *SAE International Journal of Passenger Cars*, vol. 6, no. 2, pp. 985-992, 2013

[17] F. Altiparmak, M. Gen, L. Lin, & T. Paksoy. "A genetic algorithm approach for multi-objective optimization of supply chain networks". *Computers & industrial engineering*, *51*(1), 196-215, 2006

Chapter 4
Conclusions and Future Works

In this thesis, first, we proposed a mathematical model of an Uber-like EV for optimizing its routing and charging behavior. The impact of electricity prices and passenger preference are considered. This proposed PDP-based optimization for a single EV can be extended to multiple EVs, with the emerging technologies (e.g., connected vehicles).

Second, a detailed powertrain model of a power-split HEV is proposed. The long term optimization under distance domain is performed by utilizing the EDA method. Constraints from vehicle powertrain limits, traffic conditions, and speed limits are considered. The comparison of simulation results generated by EDA and GA demonstrates the feasibility, robustness, accuracy and effectiveness of the proposed vehicle model. In addition, the proposed model can be tailored and extended with real-time implementation in the near future.

The main contributions of this master thesis are concluded as follow:

1. Introduced a mathematical model of a single frequently charged Uber-like EV;
2. Investigate the impact of electricity prices at different charging stations, and the passenger preference or requirements under certain circumstances;
3. Offered the charging station's operators with a set of total revenues under different situations and help the operators to choose an optimal charging scenario for tomorrow's operation;
4. Proposed a mathematical power-split HEV powertrain model for achieving a

5. vehicle fuel efficiency improvement;
6. Generate and optimize the vehicle speed and SOC profile under the distance domain;
7. Utilize the EDA method for solving the nonlinear, constrained complex objective function, and demonstrate the feasibility, accuracy, robustness, and effectiveness of the proposed HEV model.